ACS Catalysis

Research Article

pubs.acs.org/acscatalysis

Methanol-to-Olefins Catalysis with Hydrothermally Treated Zeolite SSZ-39

Michiel Dusselier, Mark A. Deimund, Joel E. Schmidt, and Mark E. Davis*

Chemical Engineering, California Institute of Technology, Pasadena, California 91125, United States

Supporting Information

ABSTRACT: Zeolite SSZ-39 is evaluated for catalyzing the methanol-to-olefins (MTO) reaction. By steaming NH_4−SSZ-39, Al can be removed from framework positions, resulting in an increase in framework-Si/Al_T and thus a lowered active acid site density. The Si/Al_T ratios can be controlled by the steaming temperatures. SSZ-39 steamed at 750 °C, with preserved pore volume and morphology, is an excellent MTO catalyst, as high, stable olefin selectivities, long time-on-stream activity, and low alkane production are observed. Moreover, interesting propylene/ethylene/butylene ratios of 2.8/1/1.1 are obtained, likely related to the shape of the AEI cage. By Cu^{2+}-exchanging SSZ-39, evidence is provided to show that Al_T sites in close proximity (high Al_T density) produce the unwanted effects (higher alkane-make and carbonaceous deposits) in nonsteamed materials during MTO.

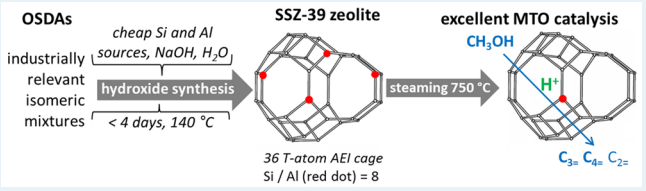

KEYWORDS: *zeolite, SSZ-39, methanol-to-olefins, heterogeneous catalysis, steaming, AEI*

INTRODUCTION

The methanol-to-olefins reaction (MTO) is an efficient and recently commercialized route to obtain ethylene and propylene.[1,2] Considering that methanol is industrially made from syngas[3] (i.e., obtainable from coal, biomass, natural gas, or oil) and that more fundamental efforts toward its direct formation from methane[4−7] or even CO_2[8] have been initiated, MTO offers a petroleum-independent route to light olefins.[9,10] The main products, propylene and ethylene, are the two most important starting products in petrochemistry for making several vital chemicals and materials such as ethylene oxide or polypropylene. The current commercial MTO catalyst is SAPO-34,[1,11] a silicoaluminophosphate molecular sieve with the CHA topology (pores consisting of 8 T atom-membered rings (8MR)). Extensive research on the conversion of MTO has been performed on zeolites (aluminosilicates) such as ZSM-5 and SSZ-13 as well,[2,12,13] and MTO catalysis similar to SAPO-34 can be obtained with (certain versions of) the latter CHA-type material.[14−18] Zeolites are more attractive catalysts in general, compared to SAPOs, because of a variety of properties including their higher (hydro)thermal stability and stronger acidity. This preference is reflected in their dominant presence in refining processes and petrochemistry.[19−23] For catalyzing the MTO reaction, a Brønsted acidic material with certain cage sizes accessible via 8MR appears to provide for the highest yields of light olefins as is consistent with the reaction pathways following the hydrocarbon pool mechanism. This mechanism has reaction pathways that, after the initial dehydration of methanol, involve an active pool of intermediates (mostly methylated benzenes) that are trapped in the cages (because they are too large to diffuse through the 8MR) and serve as a continuous source for olefin elimination and methanol addition.[12,24]

SSZ-13 uses a quaternized adamantammonium (AD) cation as the organic structure-directing agent (OSDA) in its synthesis. The preparation of this OSDA has numerous shortcomings, and AD-free routes to SSZ-13 catalysts are currently being explored.[25−27] AD-derived SSZ-13 has already been commercialized as an exhaust catalyst, as it is an excellent material for the selective reduction of NO_x (deNOx) when exchanged with Cu^{2+}.[28−32] This application is another where 8MR microporous materials show advantages.[32] Given the similar topological needs for both MTO and deNOx, it could be beneficial if one zeolite could be made into an efficient catalyst for both applications. So far, few zeolite compositions that are highly active for MTO are efficient for deNOx or vice versa, the problem being the difference in optimal Si/Al ratios for both applications. DeNOx ideally operates on zeolites with low Si/Al molar ratios (<20), in order to achieve high active site (ion-exchanged Cu) loadings,[30,33,34] whereas MTO is usually run with Si/Al ratios of over 20, owing to the increased deactivation and poor selectivities on zeolites with high Al-content.[15,26,35,36]

SSZ-39 is a zeolite with the AEI framework.[37,38] The intrazeolitic pore space of AEI consists of a three-dimensional interconnected channel system, bound by 8MR rings (3.8 × 3.8 Å) and basket-shaped cages.[39] Recently, we have shown that the hydroxide-mediated synthesis of this zeolite can be accomplished with isomeric mixtures of OSDA instead of a

Received: July 23, 2015
Revised: September 8, 2015
Published: September 17, 2015

DOI: 10.1021/acscatal.5b01577
ACS Catal. 2015, 5, 6078−6085

purified single compound.[40] These mixtures—both of structural and diastereo-isomers—naturally occur from the synthesis of the commercially relevant organic's precursors and may facilitate the large-scale cost-efficient synthesis of SSZ-39. In parallel, the conversion of FAU into AEI zeolites has been reported with tetraethylphosphonium[41] or *N*,*N*-dimethyl-3,5-dimethylpiperidinium OSDAs.[42] The hydroxide recipes typically yield materials with Si/Al molar ratios ranging from 6 to 13.[37,40,41,43] Higher Si/Al ratios (>200) have, so far, only been achieved with HF-recipes using a diethyl-quaternized OSDA.[44] Moliner et al. recently reported the use of SSZ-39 (hydroxide synthesis, Si/Al = 9, Cu^{2+}-form) for deNOx catalysis, hereby rivalling the commercial Cu-SSZ-13 catalysts, not only in activity but also in hydrothermal stability.[42,45] For the MTO catalysis, (hydroxide-derived) SSZ-39 has not been studied (aside from brief mentions in patent literature[37]).

In this work, we present a systematic study with SSZ-39 catalysts that are synthesized in hydroxide media, and we show how this zeolite with high Al content can be modified to give an efficient olefin producing catalyst by a simple steaming treatment, adding to the material's appeal. We also show how the hydrothermal stability and catalytic performance of SSZ-39 are altered by the presence of Cu^{2+}.

EXPERIMENTAL SECTION

Zeolite Synthesis. The OSDAs, 48/52 (*cis*−*trans*) or 98/2 (*cis*) mixtures of *cis*−*trans*-3,5-dimethylpiperidinium hydroxide as well as pure *cis*-2,6-dimethylpiperidinium hydroxide were donated by SACHEM Inc. in either chloride or hydroxide form. More information on these OSDAs is found in our previous publication.[40] Hydroxide ion-exchanges were performed using Dowex Marathon A (OH^-) resin. Titrations were performed using a Mettler-Toledo DL22 autotitrator using 0.01 M HCl as the titrant. The OSDA was combined with additional base (1N NaOH, RT Baker) and water in a 125 mL-Teflon Parr reactor. Then the silicon source was added, N° sodium silicate (SiO_2/Na_2O = 3.22, PQ Corporation), as well as CBV500, a NH_4−USY zeolite with Si/Al of 2.6 (Zeolyst). The synthesis gel was then manually stirred until a homogeneous white gel was obtained. The Teflon Parr reactor was then sealed and placed in a static oven at 140 °C. After 3 days of synthesis, the reactor was cooled to room temperature, the content filtered, and the resulting solids washed thoroughly with double distilled water over a Büchner setup. After drying in a 100 °C oven and equilibrating to air, the as-made materials were obtained. For *cis*−*trans*-3,5-isomer synthesis of SSZ-39, typical gel compositions were as follows: 1Si:0.033Al:0.07−0.10OSDA:0.65−0.68OH^-:0.58Na:20H_2O; with OH^- being the sum of the NaOH and OSDA(OH^-) contents, NaOH deriving from both the silica and inorganic base source and the OSDA being the 3,5-dimethylpiperidinium hydroxide. The synthesis with the *cis*-2,6 OSDA was performed similar (ESI). A small impurity, seen in PXRD, is sometimes encountered deriving from the static nature of the synthesis (tumbling synthesis can help). This can be easily removed by stirring the solid products in a 1 M HCl solution at 100 °C for 1 h (1 g per 100 mL).[40] After filtration, additional washing with water and drying, phase-pure SSZ-39 is obtained, ready for OSDA removal via calcination.

Zeolite Treatments. *Ion Exchange.* Calcined zeolites were exchanged into their NH_4^+ form by stirring them for three successive exchanges in a fresh 1 M NH_4NO_3 (1 g per 100 mL) at 100 °C for 2 h. Back-exchange with NH_4^+ of steamed, Cu-containing samples was performed identically, but at 90 °C. Cu^{2+} exchanges were performed similarly, with 0.33 M $Cu^{II}(NO_3)_2$ solutions at 90 °C, at their natural pH.

Steaming. In an MTI OTF-1200X horizontal tube furnace fitted with a 3 in. ID mullite tube under atmospheric pressure. NH_4− or Cu-SSZ-39 samples (0.5 g) were loaded in ceramic boats in the middle of the tube. The furnace was ramped at 1 °C/min to the desired steaming temperature (ranging from 550 to 1000 °C) and held there for 8 h. The furnace was fed a flow of moist air created by bubbling zero-grade air at 50 cc/min through a water saturator heated at 80 °C (corresponding to a steam partial pressure of 47.3 kPa) through the entire heating process, including ramping up and cooling-down.

Calcination. Solids were calcined in breathing grade flowing air by heating to 150 °C (1 °C·min^{-1}); holding for 3 h at 150 °C, and then heated further to 580 °C (1 °C·min^{-1}) and held for 6 h.

Catalyst and Residual Carbon-Containing Species Characterizations. ^{29}Si NMR Bloch Decay (d1 = 60s, 128 scans) was measured on a Bruker 500 MHz spectrometer in a 4 mm ZrO_2 rotor at a spinning rate of 8 kHz and referenced externally versus tetramethylsilane. Solid-state ^{27}Al MAS NMR spectra were acquired on a Bruker AM 300 MHz spectrometer operated at 78.2 MHz (90° pulse length of 2 μs, cycle delay time of 1 s, 6k scans) in a 4 mm ZrO_2 rotor at a spinning rate of 12 kHz and referenced to 1 M aq. aluminum nitrate. Before measurement, samples were hydrated overnight over a saturated KCl solution. Thermogravimetric analysis (TGA) was performed on a PerkinElmer STA 6000 with a ramp of 10 °C·min^{-1} to 900 °C under air atmosphere. This was performed on as-made zeolites to analyze the amount of OSDA included, on spent catalysts for the amount of coke included, and on MTO-ready catalysts in order to assess sorbed water content. Scanning electron microscopy (SEM) was performed on a ZEISS 1550 VP FESEM. The SEM was equipped with an Oxford X-Max SDD X-ray Energy Dispersive Spectrometer used for determining the Si, Al, and Cu contents of the samples. All powder X-ray diffraction (PXRD) characterization was conducted on a Rigaku MiniFlex II with Cu Kα radiation. All N_2-adsorption isotherms were performed at −196 °C with a Quantachrome Autosorb iQ instrument. Prior to analysis, the samples were outgassed under vacuum at 350 °C. The t-plot method was used to calculate the micropore volumes (adsorption branch). For analyzing the residual carbon-containing species occluded in spent catalysts, the postreaction zeolites were suspended in water and fully dissolved by addition of a 50 wt % HF solution, using appropriate safety precautions. After neutralization with KOH under cooling (exothermic), the hydrocarbon products were extracted with $CDCl_3$ and dried over $MgSO_4$ before ^{1}H NMR analysis on a 500 MHz Varian spectrometer.

MTO Reaction Testing. The calcined materials were pelletized, crushed, and sieved. Particles between 0.6 mm and 0.18 mm were supported between glass wool beds in an Autoclave Engineers BTRS, Jr. SS-316 tubular, continuous flow reactor. All catalysts were dried at 150 °C in situ in a 30 cm^3·min^{-1} flow of 5/95 Ar/He (V%) for 3 h and ramped to 400 °C at 1 °C/min prior to reaction. The reactions were conducted at 400 °C in a 10% methanol/inert flow. Methanol was introduced via a liquid syringe pump at 5.4 μL/min, into a gas stream of the inert blend at 30 cm^3/min. The reactant flow had a weight hourly space velocity of 1.3 h^{-1}. In a typical run, 200 mg of dry catalyst was loaded. Effluent gases were evaluated using an on-stream GC/MS (Agilent GC 6890/

DOI: 10.1021/acscatal.5b01577
ACS Catal. 2015, 5, 6078−6085

MSD5793N) with a Plot-Q capillary column. Conversions and selectivities were computed on a carbon mole basis.

RESULTS AND DISCUSSION

MTO with As-Made Materials. Initially, three typical H-SSZ-39 zeolites, made in hydroxide media with different isomeric OSDAs (*cis*-2,6-, *cis*-3,5- and *cis*−*trans*-3,5-dimethylpiperidinium hydroxide), were tested for the MTO reaction. These three materials, with Si/Al ratios between 8 and 9, behaved comparably, consistent with their similar physicochemical characterization (Supporting Information, Figures S1−S4) and our earlier report.[40] A typical reaction profile (Figure 1 for *cis*−*trans*-3,5 OSDA, Supporting Information Figures S5,S6 for other isomers) reveals MTO catalysis with (i) an initially very high C_1 - C_4 alkane production (mainly propane), (ii) time-dependent olefin selectivities, and (iii) relatively fast deactivation, with the conversion dropping below 80% after 135 min on stream. These three features render optimal MTO catalysis difficult (e.g., high alkane make is not desirable).

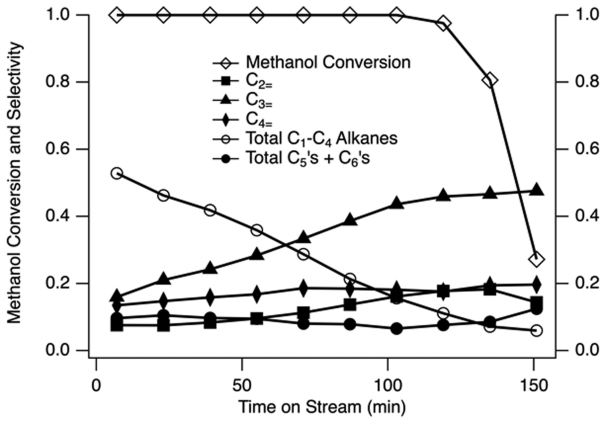

Figure 1. Methanol conversion and product profiles with H-SSZ-39, Si/Al = 8.5, from a *cis*−*trans*-3,5 OSDA synthesis.

The fast deactivation points to the formation of large amounts of carbon deposits that eventually fill the pores.[2,16,32] TGA analysis of the spent catalyst indeed revealed the presence of 21 wt % of organic material. The deactivation is likely connected to the high alkane production because the presence of saturated hydrocarbons requires hydrogen that evolves from the formation of dehydrogenated, unsaturated aromatic species. Deactivation due to active site destruction or structural collapse seemed unlikely, as PXRD traces, ^{29}Si and ^{27}Al NMR spectra, as well as micropore volumes, all measured after calcination of the spent catalyst (of Figure 1) were virtually identical to the fresh catalyst (Supporting Information Figure S7). These three MTO trends are thus connected and likely find their origin in the high acid-site density of the material.[15,35] Recently, we noticed that, with a series of SSZ-13 catalysts with increasing Si/Al ratios (spanning from 5 to 55), the MTO performance was improved (lower alkane make, constant olefin selectivities, and longer times-on-stream) with higher Si/Al ratios.[15] Furthermore, we reported that zeolites with the CHA topology and low Si/Al (ca. below 5) from OSDA-free synthesis could have improved MTO performance by steaming to raise the framework Si/Al ratio.[26] For SSZ-39 with Si/Al = 8, approximately 4 aluminum atoms should be present per cage (shared over 3 cages). By analogy to SSZ-13 (built from double-6MR units as well), this low Si/Al provides Al sites in close proximity.[34] Given that the hydroxide route for synthesizing SSZ-39 produces materials within a very limited range of Si/Al ratios,[40,45] we explored methods to postsynthetically alter SSZ-39.

Cu^{2+} Exchange and Steaming of SSZ-39. Cu^{2+}-exchange and steaming was investigated in order to test whether postsynthetic alterations in the framework composition affect MTO performance. Steaming is known to remove Al_T from zeolite frameworks by hydrolysis and creates pentacoordinated and octahedral species. With 8MR zeolites, the extra-framework (hydrated) aluminums cannot be removed due to their size.[26,44] However, whereas the bulk Si/Al ratio is not changed, steaming can effectively enhance the Si/Al_T ratio, with Al_T being the tetrahedrally coordinated framework aluminum that gives acidity. We conducted a series of experiments to explore the effect of steaming at 750 °C. In addition, SSZ-39 was exchanged with divalent Cu^{2+} (Figure 2), as would be done

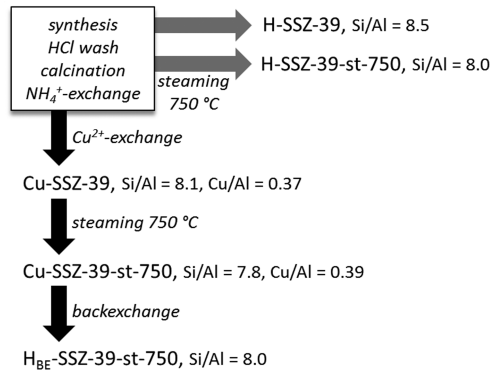

Figure 2. Experimental treatments and the corresponding elemental Cu/Al and Si/Al ratios with SSZ-39. All samples calcined before MTO reaction.

to create a deNOx catalyst. Ideally, divalent species should only exchange with two Al sites that are sufficiently close to one another (e.g., opposite to each other in a 6MR ring).[46] The copper loading of our sample of SSZ-39 is 0.37 Cu/Al. Therefore, about 26% of the Al_T (likely isolated) should still be balanced by an acidic proton. The Cu-exchanged SSZ-39 was steamed in order to probe whether framework aluminum that provided for copper exchange would remain after steaming. As reported previously, a partially exchanged SSZ-39 sample had an enhanced steaming-stability when compared to a fully exchanged sample and kept about 93% of its micropore volume (the Cu/Al = 0.5 sample was detrimentally effected by steaming, with only 32% of its pore volume remaining).[45] After steaming the Cu-exchanged sample, it was back-exchanged with NH_4^+. The back-exchange was able to remove all of the copper and enables evaluation of this MTO catalyst in its strictly acidic form (H_{BE}-SSZ-39-st-750, Si/Al = 8). To summarize our materials, five SSZ-39 catalysts were prepared to probe the influence of: (i) steaming on MTO catalysis, (ii) Cu^{2+} protection of framework Al sites with close proximity during steaming, (iii) Cu^{2+} protection of framework Al sites with close proximity during MTO, and (iv) Cu^{2+} protected steaming of SSZ-39 on MTO in the absence of Cu^{2+}.

Characterizations of these materials included PXRD for the full series (Supporting Information Figure S8) and ^{27}Al NMR, ^{29}Si NMR (Figure 3), and N_2-physisorption for the three key (H-form) materials (Figure S9). The NMR data and the

DOI: 10.1021/acscatal.5b01577
ACS Catal. 2015, 5, 6078−6085

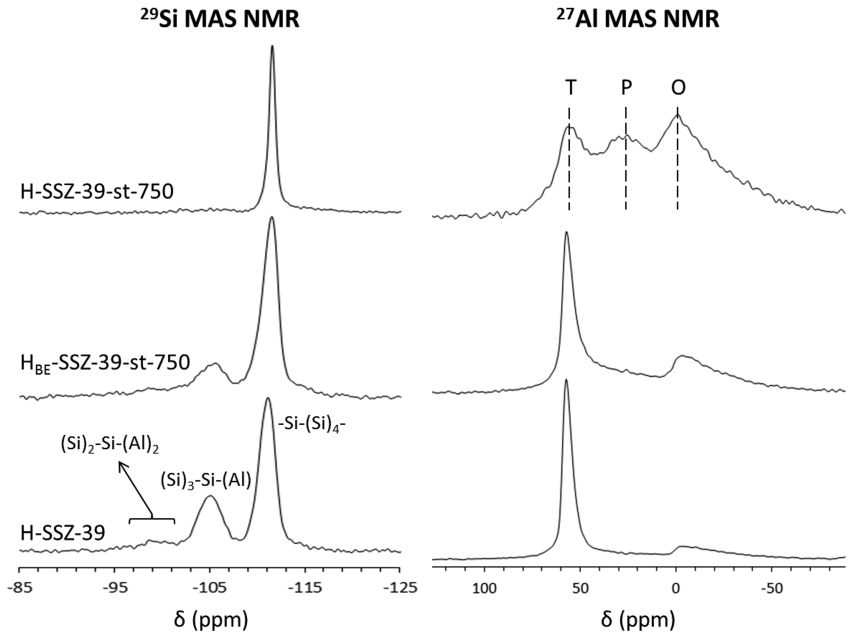

Figure 3. ^{29}Si and ^{27}Al MAS NMR spectra for as-made, back-exchanged, and steamed samples of SSZ-39, as described in Figure 2. Al environments of steamed sample: T = tetrahedral, P = pentacoordinated, O = octahedral, deconvoluted: T/P/O = 13/18/69.

adsorption properties of the Cu-containing materials should be similar to either H-SSZ-39 or H_{BE}-SSZ-39-st-750. PXRD revealed no significant differences in the series of SSZ-39s (phase-pure AEI), with the exception of notable shifts toward lower *d*-spacings in H-SSZ-39-st-750 (detailed in Figure S8), indicating a smaller unit cell. Unit cell size is directly linked with the Al-content of zeolite frameworks (e.g., well documented for USY zeolites).[47]

The removal of Al_T atoms was confirmed by ^{27}Al and ^{29}Si NMR data, the former showing that roughly 13% of all Al remained in the framework after steaming (tetrahedral, Figure 3), whereas the latter hardly detected $(Si)_3$-Si-(Al) signals, when compared to the control H-SSZ-39. An effective Si/Al_T ratio of about 62 can be calculated for the steamed material, by combining results from the bulk Si/Al ratio and ^{27}Al NMR. This ratio gives an (acidic) Al_T distribution of ±0.57 Al_T-atoms per cage (of 36 T atoms, shared over three cages). Importantly, the steaming treatment did not affect the pore volume compared to the control (Supporting Information Figure S9), as a similar 0.23 $cm^3\ g^{-1}$ was analyzed. The material steamed in the presence of Cu^{2+} (measured after back-exchange), gave very different NMR spectra that clearly indicated that the divalent ion stabilized the framework Al during steaming. Compared to the control, only a small increase in extra-framework Al was found (paralleled by a small decrease in the $(Si)_3$-Si-(Al) signal relative to the other signals). Interestingly, the $(Si)_2$-Si-$(Al)_2$ signal, assigned to bridged Al sites, did not seem to decrease (detail in Supporting Information Figure S10). Compared to the steaming in absence of copper, it is clear that a large part of the Al_T has been stabilized. This is also of importance in deNOx catalysis that requires operation at elevated temperatures in the presence of water (formed in situ).[45] Logically, the pore volume of the steamed Cu-stabilized material was preserved as well (Figure S9).

The steamed zeolite, H-SSZ-39-st-750, gave excellent MTO catalysis (Figure 4); the deactivation was very slow, less than 10% of alkanes were formed, and stable, high olefin selectivities were measured. The propylene/ethylene/butylene ratios at

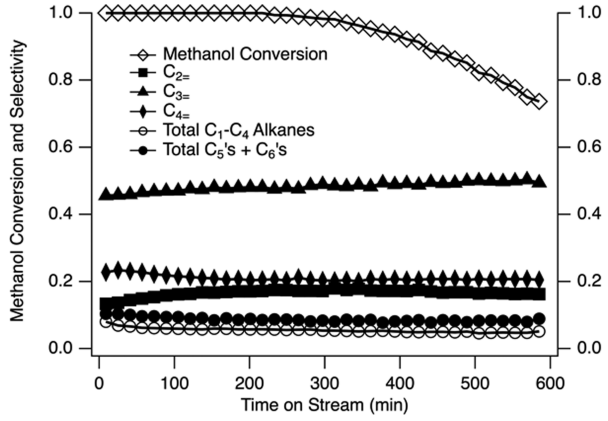

Figure 4. MTO result of H-SSZ-39-st-750; note time scale.

maximum olefin yield were 2.8/1/1.1. These ratios are very interesting, given the fact that ethylene has the lowest value of these three light olefins and the rising need for propylene and butylenes due to changes in feedstock-dependent steam-cracker production.[48] The MTO behavior of the steamed zeolite was compared to that of an SSZ-13 zeolite with similar Si/Al_T ratio (~55, nonsteamed, AD-synthesis). This zeolite had comparable alkane and time-on-stream features but a 0.8/1/0.3 propylene/ethylene/butylene ratio (Supporting Information Figure S11),[15] in line with the literature.[14,16] Comparably, the industrial catalyst, SAPO-34 (CHA), is known to produce olefins within a (condition-dependent[11]) limited range of propylene/ethylene ratios near 1.[16,49] For benchmarking reasons, we also tested a homemade SAPO-34 catalyst in our setup (Supporting Information Figure S12) and indeed noted a 1.15/1/0.4 ratio, similar to the aluminosilicate CHA above (SSZ-13) and confirming the unique C3- and C4-olefin-favoring behavior of SSZ-39. Comparing SSZ-39 to SAPO-18, a known MTO catalyst in literature with the same AEI topology,[50,51] shows that their selectivity trend is similar: more propylene than ethylene and a significant butylene

DOI: 10.1021/acscatal.5b01577
ACS Catal. 2015, 5, 6078−6085

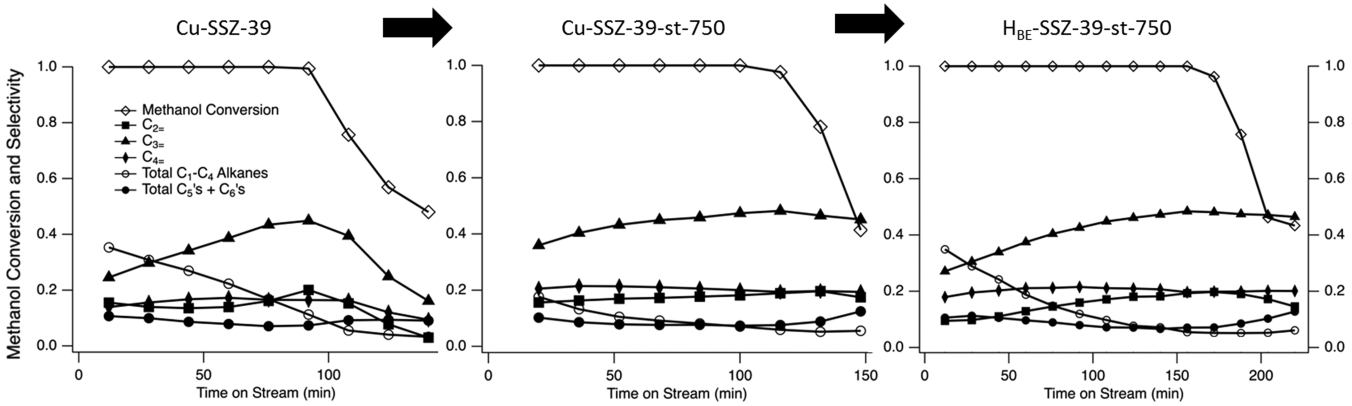

Figure 5. MTO reaction results for SSZ-39 samples involving Cu^{2+} described in Figure 2.

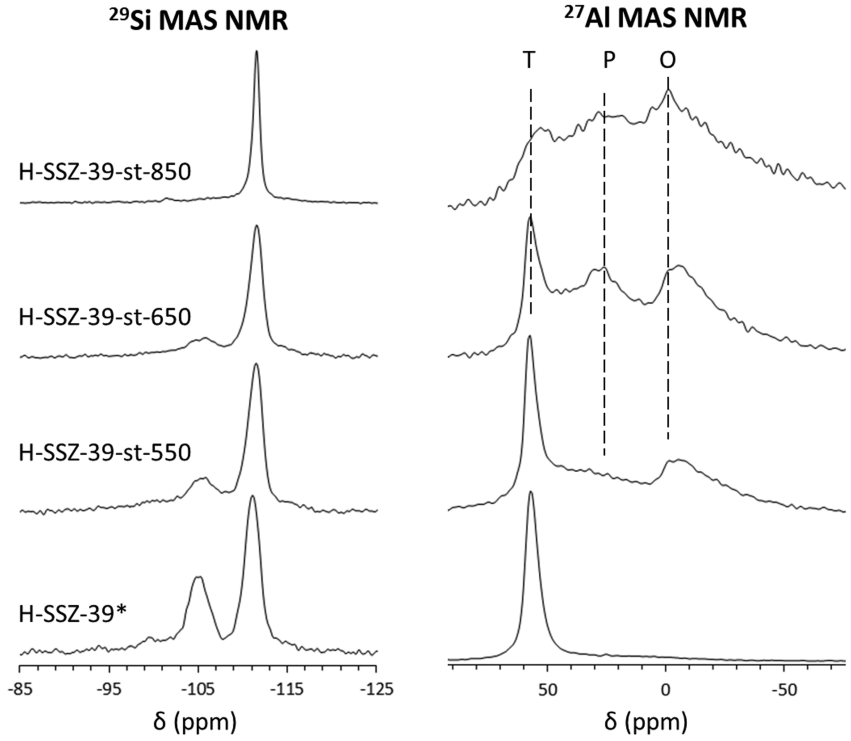

Figure 6. ^{29}Si and ^{27}Al MAS NMR of samples steamed at different temperatures. * different batch than H-SSZ-39 in Figure 3. H-SSZ-39-st-750 fits well in the trend.

production, although the trend is even more pronounced for the zeolite. Literature suggests that differences in the shape of the cage are responsible for the change in selectivity between SAPO-34 and SAPO-18, as the AEI cage is basket-shaped and wider at the bottom than the more symmetric CHA cage.[50−52] Our SSZ-39 results (with direct SSZ-13 comparison) thus indicate that this selectivity trend exists as well for aluminosilicate compositions of these microporous frameworks, although even more in relative excess of larger olefins. While the alkene methylation/cracking mechanism cannot be excluded, the trend could be caused by cage-related differences in the polymethylbenzene intermediates of the hydrocarbon pool mechanism (as in SAPO-18).[51] The presence of some alkylated (poly)aromatic species (occluded carbon analysis, see below and Supporting Information) hints to this, but a mechanistic study would need to confirm this.

The steamed SSZ-39's selectivities are very similar to those in the unsteamed MTO profile at its propylene maximum (seemingly Si/Al$_T$-independent, Figure 1) but without the high initial alkane formation and fast deactivation. The high density of framework acid sites in the unsteamed SSZ-39 appear to be causing the production of alkanes and concomitant carbon deposition that leads to a fast deactivation. The MTO results from the series of SSZ-39 samples that involved the presence of copper (series in Figure 2) allow further investigation of the origins of these effects. Compared to the unsteamed SSZ-39 (Figure 1), Cu-exchanged SSZ-39 (Figure 5) shows a lowered initial alkane production (from 53 to ±40%). The Cu^{2+} ions, which preferably exchange with two closely related Al sites, slightly hinder alkane production. We hypothesize that this decrease is not as large as it could be, due to the dynamic nature of such ion-exchanged species at these temperatures, as recently postulated for Cu-exchanged species on SSZ-13 zeolites in deNOx catalysis conditions.[53] Cu-SSZ-39-st-750 shows an improved MTO profile, and the main differences with Cu-SSZ-39 are the lower degree of variations

DOI: 10.1021/acscatal.5b01577
ACS Catal. 2015, 5, 6078−6085

with time-on-stream and an even further lowering of alkane formation (<20% initially). This correlates well with the observed stability during steaming of a large part of the tetrahedral Al when Cu was present (Figure 3), and hints to fact the Cu-exchanged aluminum sites that are in close proximity to each other are still present in the material. If so, we expect that after exchanging the Cu away, the transient nature and high alkane production should return. Indeed, in its proton form, the H_{BE}-SSZ-39-st-750 catalyst again produces nearly 40% of alkanes initially, but compared to the control H-SSZ-39 catalyst, it has a longer active time-on-stream (consistent with the minor Al_T removal, Figure 3). Thus, the MTO results from the use of copper exchange, steaming, and back-exchange strongly suggest that the high initial alkane production (and related deactivation) in as-made SSZ-39 catalysts is caused by the presence of closely associated (e.g., bridged) Al_T sites. The differences in MTO when comparing H_{BE}-SSZ-39-st-750 (Figure 5, right) with the (NH_4-form) steamed SSZ-39 (Figure 4), clearly show the effects of Cu-presence during steaming. In the case of steaming without Cu, it is likely that closely associated Al sites are more prone to dealumination than isolated sites, but this is hard to evidence due to the possibility of Si-migration and healing.[26,54,55]

Effects of the Steaming Temperature on MTO. As the steaming treatment at 750 °C, in absence of copper, transformed SSZ-39 into an interesting MTO catalyst, the effect of steaming temperature was explored. A batch of NH_4−SSZ-39 (*cis*−*trans*-3,5 OSDA, Si/Al 10.9, 0.23 $cm^3.g^{-1}$) was steamed at three additional temperatures, namely, 550, 650, and 850 °C. All resulting materials showed the same PXRD pattern (Supporting Information Figure S13) and a similar *d*-spacing shift, as noted above, was observed with H-SSZ-39-st-850. The micropore volume of the latter material was measured at 0.21 $cm^3{\cdot}g^{-1}$, indicating no sign of structural collapse. The solid-state ^{29}Si and ^{27}Al NMR spectra of these materials (Figure 6) showed a gradual Al_T removal with higher temperatures and an increase in octahedral and pentacoordinated species. The T/P/O ratio of the steamed catalysts, as well as the key MTO reaction data from these three materials, are summarized in 6Table 1 (MTO reaction plots provided in Supporting Information Figures S14−16), along with the previous MTO data (Figures 1 and 4).

These reaction data are consistent with the trends in the characterization data: H-SSZ-39-st-550 showed some improvement over the as-made materials, but in line with its intermediate Si/Al_T ratio, viz., 37, still produced about 34% of alkanes initially, followed by transient olefin profiles and a medium fast deactivation ($t_{80\%}$ = 175 min). After steaming at 650 °C, more framework Al_T is removed, and thus, better MTO features were noted, albeit less pronounced than the previously mentioned 750 °C sample. For the catalyst steamed at 850 °C, the selectivities were similar to those from the 750 °C steamed material (few alkanes), but a fast deactivation occurred (Table 1, 80 min). This is likely caused by the lack of sufficient active sites remaining after the steaming, as the Si/Al_T ratio is 124. We confirmed such deteriorated catalysis at elevated steaming temperatures, with a sample of SSZ-39 (made with the *cis*-3,5 OSDA, Figure S1) steamed at 900 °C (MTO, Supporting Information Figure S17). Steaming NH_4−SSZ-39 at 1000 °C rendered an X-ray amorphous material (Figure S1). An optimal steaming temperature thus appears to be around 750 ± 50 °C. Improved MTO catalysis after steaming at 750 °C was confirmed with SSZ-39 samples made with *cis*-3,5 and *cis*-2,6 OSDAs as well (Supporting Information Figures S18,S19).

In addition to catalytic applications like MTO, steamed SSZ-39 zeolites could be useful in other applications such as gas separation and adsorption.[32] Importantly, the pore volume of the materials seems to be preserved in steaming up to 850 °C, as does its morphology (Figure 7).

Table 1. Effect of Steaming Temperature on MTO Catalysis with SSZ-39[a]

T [°C]	T/P/O[b]	alkane yield[c]	$C_{2=}$ [%]	$C_{3=}$ [%]	$C_{4=}$ [%]	$t_{80\%}$[d] [min]
/ [#]	-	53	16	43	18	135
550	27/30/44	34	21	48	19	175
650	15/35/50	16	18	48	20	190
750[#]	13/18/69	8	17	48	20	520
850	8/16/76	6	14	48	20	80

[a]Respective olefin selectivities at maximum $C_{3=}$ yield and full MeOH conversion. [b]Distribution of Al environments of steamed samples by deconvolution of −57 ppm (T), −30 ppm (P), and 0 ppm (O) signals in ^{27}Al NMR. [c]Initial alkane selectivity (%, first measured point). [d]Time-on-stream when the conversion drops to 80%. / = nonsteamed control. [#] Other batch of SSZ-39 (from Figures 1−4, bulk Si/Al 8).

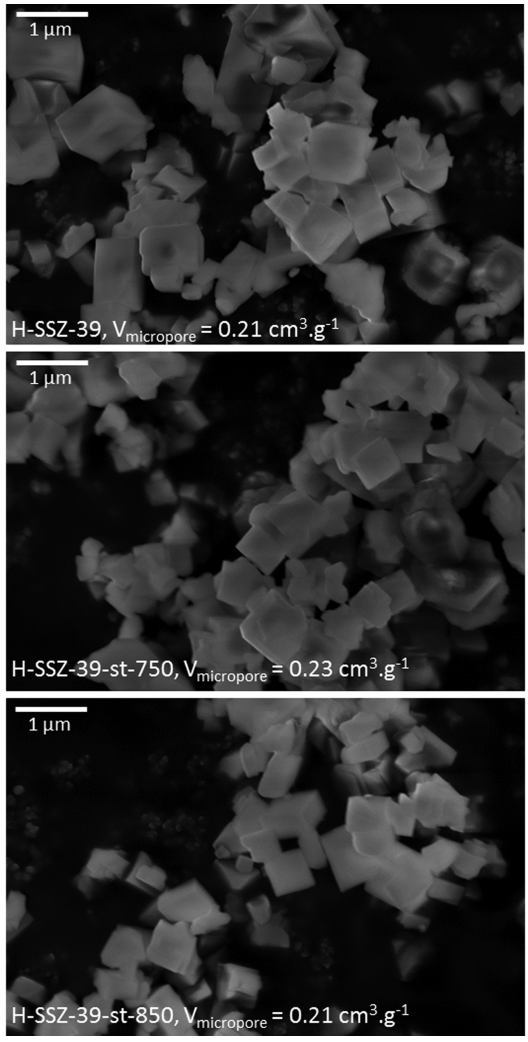

Figure 7. SEM images of nonsteamed and steamed SSZ-39.

DOI: 10.1021/acscatal.5b01577
ACS Catal. 2015, 5, 6078−6085

Steaming of SSZ-39 thus creates microporous AEI materials with tunable Si/Al_T, which is controlled by the steaming temperature. It should be noted that for all steamed samples, the bulk Si/Al ratios of the precursor was preserved (i.e., around 8−10) and that mesopore formation was not detected.

Residual Carbon-Containing Species and Zeolite Reuse. We analyzed the residual carbon-containing species occluded in spent zeolites by TGA and ^1H NMR (after dissolution of the aluminosilicate framework), and the results are provided in the Supporting Information (Figure S20). Briefly, ca. 20 wt % of carbon-containing species, of mostly aromatic nature, was obtained for nearly all fast deactivating catalysts, except for H-SSZ-st-850. Likely, the latter material deactivates quickly due to its lack of sufficient active sites ($Si/Al_T > 100$), which is confirmed by the low residual carbon content (7 wt %). An optimal steamed SSZ-39 (750 °C, *cis*-2,6) contained 13 wt % of carbonaceous deposits

Finally, the optimal catalyst (Figure 7, H-SSZ-39-st-750) was reused for two additional, consecutive MTO reactions (Supporting Information Figure S21). Without searching for an optimal regeneration strategy, a simple intermittent dry calcination was used. Although the time-on-stream shortens somewhat in the consecutive runs, the olefin production immediately starts up again, at selectivities identical to those in the first run. Over three runs, the catalyst had efficiently converted methanol ($X > 80\%$) for about 17 h on stream at 400 °C.

SUMMARY

We report the first systematic study on catalyzing the methanol-to-olefins reaction with SSZ-39 zeolites, obtained from hydroxide media. These zeolites, accessible from mixtures of isomeric OSDAs in low Si/Al ratios (<11),[40] are known as efficient deNOx catalysts, when exchanged with Cu^{2+}.[45] In their acidic form, however, the zeolites are not suited for catalyzing the MTO reaction, due to their fast deactivation, high alkane make and time-dependent olefin selectivities. These three connected features are caused by the high framework aluminum (Al_T) density and thus too closely associated acid sites (likely bridging). With a simple steaming treatment at 750 °C, the Al-dense zeolites (NH_4^+-form) can be transformed into effective olefin-producing catalysts. The steaming removes Al from framework positions but does not cause structural collapse as both pore volume and morphology were preserved up to at least 850 °C. The Si/Al_T ratio increase can be controlled by the steaming temperatures and enables efficient MTO catalysis with SSZ-39 (Si/Al_T between 50 and 100). Furthermore, we noticed that steaming in the presence of Cu^{2+} does not remove the unwanted closely related Al_T atoms, which allows the alkane production to come right back after proton-exchange. Optimally (NH_4-form) steamed SSZ-39 zeolites have long time-on-stream stability, are 85% selective toward olefins at full methanol conversion, and display very unique propylene/ethylene/butylene ratios of 2.8/1/1.1. This behavior in favor of higher olefins (compared to CHA systems e.g.) is likely related to the basket-shape of the AEI cage (seen in Figure 8). It is recognized that both efficient MTO and deNOx catalysts can be obtained from one zeolite synthesis, given the use of respectively postsynthetic steaming (this work) or Cu-exchange (literature) (Figure 8).

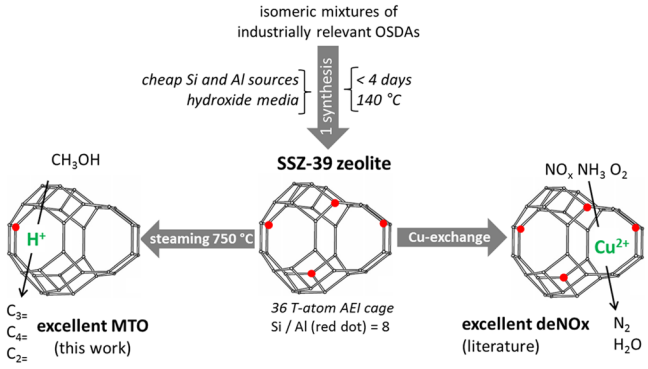

Figure 8. Overview of our MTO work in the context of recent progress in literature on deNOx[42,45] and SSZ-39 synthesis.[40,42] Cx= represents an olefin with x carbon atoms. Each T atom is shared between three cages.[56] The deNOx materials in the literature are very similar (e.g., Cu/Al and Si/Al-wise) to ours (Figure 2).

ASSOCIATED CONTENT

Supporting Information

The Supporting Information is available free of charge on the ACS Publications website at DOI: 10.1021/acscatal.5b01577.

Additional PXRD; solid-state NMR; N_2-physisorption, ^1H NMR, TGA, and MTO reaction data (PDF)

AUTHOR INFORMATION

Corresponding Author

*E-mail: mdavis@cheme.caltech.edu.

Notes

The authors declare no competing financial interest.

ACKNOWLEDGMENTS

M.D. acknowledges Research Foundation − Flanders, Belgium (FWO) for his postdoctoral funding and the Belgian American Educational Foundation (honorary fellow, boat of 2014). M.A.D. thanks The Dow Chemical Company for financial support. J.E.S. would like to thank the NDSEG for their support through a fellowship. PQ Corporation is thanked for providing us with sodium silicate and SACHEM inc. is thanked for providing the OSDAs.

NOMENCLATURE

Si/Al ratio, molar silicon/aluminum ratio; H-SSZ-39, SSZ-39 zeolite in its proton (H^+) form, after successive washing, HCl-treatment, calcination, NH_4^+-exchange and calcination; H-SSZ-39-st-750, as H-SSZ-39, with the addition of steaming at 750 °C after NH_4^+-exchange; Cu-SSZ-39, as H-SSZ-39, with the addition of Cu^{2+} exchange after NH_4^+-exchange; Cu-SSZ-39-st-750, as Cu-SSZ-39, with the addition of steaming at 750 °C after Cu-exchange; H_{BE}-SSZ-39-st-750, as Cu-SSZ-39-st-750, with the addition of back-exchange to NH_4^+-form after steaming

REFERENCES

(1) Tian, P.; Wei, Y.; Ye, M.; Liu, Z. *ACS Catal.* **2015**, *5*, 1922−1938.
(2) Stöcker, M. *Microporous Mesoporous Mater.* **1999**, *29*, 3−48.
(3) Behrens, M.; Studt, F.; Kasatkin, I.; Kühl, S.; Hävecker, M.; Abild-Pedersen, F.; Zander, S.; Girgsdies, F.; Kurr, P.; Kniep, B.-L.; Tovar, M.; Fischer, R. W.; Nørskov, J. K.; Schlögl, R. *Science* **2012**, *336*, 893−897.

DOI: 10.1021/acscatal.5b01577
ACS Catal. 2015, 5, 6078−6085

(4) Groothaert, M. H.; Smeets, P. J.; Sels, B. F.; Jacobs, P. A.; Schoonheydt, R. A. *J. Am. Chem. Soc.* **2005**, *127*, 1394−1395.
(5) Hammond, C.; Forde, M. M.; Rahim, A.; Hasbi, M.; Thetford, A.; He, Q.; Jenkins, R. L.; Dimitratos, N.; Lopez-Sanchez, J. A.; Dummer, N. F.; et al. *Angew. Chem., Int. Ed.* **2012**, *51*, 5129−5133.
(6) Wulfers, M. J.; Teketel, S.; Ipek, B.; Lobo, R. F. *Chem. Commun.* **2015**, *51*, 4447−4450.
(7) Woertink, J. S.; Smeets, P. J.; Groothaert, M. H.; Vance, M. A.; Sels, B. F.; Schoonheydt, R. A.; Solomon, E. I. *Proc. Natl. Acad. Sci. U. S. A.* **2009**, *106*, 18908−18913.
(8) Barton, E. E.; Rampulla, D. M.; Bocarsly, A. B. *J. Am. Chem. Soc.* **2008**, *130*, 6342−6344.
(9) Olah, G. A.; Goeppert, A.; Prakash, G. S. *Beyond oil and gas: the methanol economy*; John Wiley & Sons: Hoboken, NJ, 2011.
(10) Olah, G. A. *Angew. Chem., Int. Ed.* **2005**, *44*, 2636−2639.
(11) Barger, P. In *Zeolites for cleaner technologies*; Guisnet, M., Gilson, J.-P., Eds.; Imperial College Press: London, 2002.
(12) Olsbye, U.; Svelle, S.; Bjørgen, M.; Beato, P.; Janssens, T. V. W.; Joensen, F.; Bordiga, S.; Lillerud, K. P. *Angew. Chem., Int. Ed.* **2012**, *51*, 5810−5831.
(13) Almutairi, S. M. T.; Mezari, B.; Pidko, E. A.; Magusin, P. C. M. M.; Hensen, E. J. M. *J. Catal.* **2013**, *307*, 194−203.
(14) Bhawe, Y.; Moliner-Marin, M.; Lunn, J. D.; Liu, Y.; Malek, A.; Davis, M. *ACS Catal.* **2012**, *2*, 2490−2495.
(15) Deimund, M. A.; Harrison, L.; Lunn, J. D.; Liu, Y.; Malek, A.; Davis, M. E. *in revision stage at ACS Catal*, **2015**
(16) Bleken, F.; Bjørgen, M.; Palumbo, L.; Bordiga, S.; Svelle, S.; Lillerud, K.-P.; Olsbye, U. *Top. Catal.* **2009**, *52*, 218−228.
(17) Zhu, Q.; Kondo, J. N.; Ohnuma, R.; Kubota, Y.; Yamaguchi, M.; Tatsumi, T. *Microporous Mesoporous Mater.* **2008**, *112*, 153−161.
(18) Wu, L.; Degirmenci, V.; Magusin, P. C. M. M.; Lousberg, N. J. H. G. M.; Hensen, E. J. M. *J. Catal.* **2013**, *298*, 27−40.
(19) Vermeiren, W.; Gilson, J. P. *Top. Catal.* **2009**, *52*, 1131−1161.
(20) Jacobs, P. A.; Dusselier, M.; Sels, B. F. *Angew. Chem., Int. Ed.* **2014**, *53*, 8621−8626.
(21) Corma, A. *Chem. Rev.* **1995**, *95*, 559−614.
(22) Corma, A. *Chem. Rev.* **1997**, *97*, 2373−2420.
(23) Dusselier, M.; Van Wouwe, P.; Dewaele, A.; Jacobs, P. A.; Sels, B. F. *Science* **2015**, *349*, 78−80.
(24) Song, W.; Haw, J. F.; Nicholas, J. B.; Heneghan, C. S. *J. Am. Chem. Soc.* **2000**, *122*, 10726−10727.
(25) Martin, N.; Moliner, M.; Corma, A. *Chem. Commun.* **2015**, *51*, 9965−9968.
(26) Ji, Y.; Deimund, M. A.; Bhawe, Y.; Davis, M. E. *ACS Catal.* **2015**, *5*, 4456−4465.
(27) Yilmaz, B.; Berens, U.; Swaminathan, V. N.; Müller, U.; Iffland, G.; Szarvas, L.; US, Ed. 2012.
(28) Kwak, J. H.; Tonkyn, R. G.; Kim, D. H.; Szanyi, J.; Peden, C. H. F. *J. Catal.* **2010**, *275*, 187−190.
(29) Lambert, C.; Cavataio, G. In *Urea-SCR Technology for deNOx After Treatment of Diesel Exhausts*; Nova, I., Tronconi, E., Eds.; Springer: New York, 2014; pp 659−689.
(30) Beale, A. M.; Gao, F.; Lezcano-Gonzalez, I.; Peden, C. H. F.; Szanyi, J. *Chem. Soc. Rev.* **2015**, DOI: 10.1039/C5CS00108K.
(31) Borfecchia, E.; Lomachenko, K. A.; Giordanino, F.; Falsig, H.; Beato, P.; Soldatov, A. V.; Bordiga, S.; Lamberti, C. *Chem. Sci.* **2015**, *6*, 548−563.
(32) Moliner, M.; Martínez, C.; Corma, A. *Chem. Mater.* **2014**, *26*, 246−258.
(33) Paolucci, C.; Verma, A. A.; Bates, S. A.; Kispersky, V. F.; Miller, J. T.; Gounder, R.; Delgass, W. N.; Ribeiro, F. H.; Schneider, W. F. *Angew. Chem., Int. Ed.* **2014**, *53*, 11828−11833.
(34) Bates, S. A.; Delgass, W. N.; Ribeiro, F. H.; Miller, J. T.; Gounder, R. *J. Catal.* **2014**, *312*, 26−36.
(35) Kumita, Y.; Gascon, J.; Stavitski, E.; Moulijn, J. A.; Kapteijn, F. *Appl. Catal., A* **2011**, *391*, 234−243.
(36) Schmidt, J. E.; Deimund, M. A.; Davis, M. E. *Chem. Mater.* **2014**, *26*, 7099−7105.
(37) Zones, S. I.; Nakagawa, Y.; Evans, S. T.; Lee, G. S. U.S. Patent 5,958,370, 1999.
(38) Wagner, P.; Nakagawa, Y.; Lee, G. S.; Davis, M. E.; Elomari, S.; Medrud, R. C.; Zones, S. I. *J. Am. Chem. Soc.* **1999**, *122*, 263−273.
(39) IZA-Structure-Commission. *Database of Zeolite Structures*. http://www.iza-online.org/.
(40) Dusselier, M.; Schmidt, J. E.; Moulton, R.; Haymore, B.; Hellums, M.; Davis, M. E. *Chem. Mater.* **2015**, *27*, 2695−2702.
(41) Maruo, T.; Yamanaka, N.; Tsunoji, N.; Sadakane, M.; Sano, T. *Chem. Lett.* **2014**, *43*, 302−304.
(42) Martin, N.; Boruntea, C. R.; Moliner, M.; Corma, A. *Chem. Commun.* **2015**, *51*, 11030−11033.
(43) Schmidt, J.; Deem, M.; Lew, C.; Davis, T. *Top. Catal.* **2015**, *58*, 410−415.
(44) Cao, G.; Strohmaier, K. G.; Li, H.; Guram, A. S.; Saxton, R. J.; Muraoka, M. T.; Yoder, J. C.; Yaccatu, K. Patent WO2005063624A1, 2005.
(45) Moliner, M.; Franch, C.; Palomares, E.; Grill, M.; Corma, A. *Chem. Commun.* **2012**, *48*, 8264−8266.
(46) Bates, S. A.; Verma, A. A.; Paolucci, C.; Parekh, A. A.; Anggara, T.; Yezerets, A.; Schneider, W. F.; Miller, J. T.; Delgass, W. N.; Ribeiro, F. H. *J. Catal.* **2014**, *312*, 87−97.
(47) *Introduction to Zeolite Science and Practice*, 2nd ed.; H. van Bekkum, Flanigen, E. M., Jacobs, P. A., Jansen, J. C., Eds.; Elsevier: Amsterdam, 2001.
(48) Bruijnincx, P. C. A.; Weckhuysen, B. M. *Angew. Chem., Int. Ed.* **2013**, *52*, 11980−11987.
(49) Vora, B.; Marker, T.; Barger, P.; Nilsen, H.; Kvisle, S.; Fuglerud, T. *Stud. Surf. Sci. Catal.* **1997**, *107*, 87−91.
(50) Smith, R. L.; Svelle, S.; Del Campo, P.; Fuglerud, T.; Arstad, B.; Lind, A.; Chavan, S.; Attfield, M. P.; Akporiaye, D.; Anderson, M. W. *Appl. Catal., A* **2015**, *505*, 1−7.
(51) Chen, J.; Li, J.; Yuan, C.; Xu, S.; Wei, Y.; Wang, Q.; Zhou, Y.; Wang, J.; Zhang, M.; He, Y.; Xu, S.; Liu, Z. *Catal. Sci. Technol.* **2014**, *4*, 3268−3277.
(52) Marcus, D. M.; Song, W.; Ng, L. L.; Haw, J. F. *Langmuir* **2002**, *18*, 8386−8391.
(53) Göltl, F.; Sautet, P.; Hermans, I. *Angew. Chem., Int. Ed.* **2015**, *54*, 7799−7804.
(54) Lutz, W. *Adv. Mater. Sci. Eng.* **2014**, [Online] http://dx.doi.org/10.1155/2014/724248.
(55) Lago, R. M.; Haag, W. O.; Mikovsky, R. J.; Olson, D. H.; Hellring, S. D.; Schmitt, K. D.; Kerr, G. T. *Stud. Surf. Sci. Catal.* **1986**, *28*, 677−684.
(56) First, E. L.; Gounaris, C. E.; Wei, J.; Floudas, C. A. *Phys. Chem. Chem. Phys.* **2011**, *13*, 17339−17358.

DOI: 10.1021/acscatal.5b01577
ACS Catal. 2015, 5, 6078−6085